

## **ADSORPTION OF CONGO RED USING CHITOSAN MONTMORILLONITE IN BATCH AND COLUMN METHOD**

**RISKIONO SLAMET & ERDAWATI**

Chemistry Department, State University of Jakarta, Jalan Pemuda No 10, Rawamangun, Jakarta Timur, Indonesia

### **ABSTRACT**

The synthesis, characterization and application of chitosan/montmorillonite (Chi-MMT) for adsorption Congo red using batch and column method. The adsorbents were characterized by using Fourier transform infrared spectroscopy (FTIR), BET and XRD. Congo red was adsorbed under different operating conditions such as flow rate and mass sorbent. At lower flow rate, the quantity of treated water and adsorption capacity were found to increase. At higher mass sorbent, better adsorption capacity was observed. The theoretical service times evaluated from Thomas model for different flow rates and mass sorbent shows good correlation with the experimental data. Column regeneration, dye recovery and the possibility of reusing the regenerated Chi-MMT were also investigated.

**KEYWORDS:** Chi-MMT, Congo Red, Adsorption, Column Method, Thomas Model

### **INTRODUCTION**

Synthetic dyes are extensively used in textile industries and wastewater discharged from these industries are usually polluted by dyes. Effluents from the textile industries are main source of water pollution, because dyes in waste water undergo chemical as well as biological changes, and consume dissolved oxygen. Its strong color characteristic, high BOD and COD and destroy aquatic life (Crini, 2006). Researchers have also determined that some dyes and their degradation products can be mutagenic and carcinogenic (Lourenco et al, 2003). Therefore, it is necessary to treat textile effluents prior to their discharge into the receiving water. This study focuses on understanding bioadsorption process and developing a cost effective technology for treatment of effluents from textile industries.

Various methods of dye removal have been studied and developed including physical, chemical, physico-chemical and biological methods (Pearce et al, 2003). Adsorption is a conventional treatment technique, but efficient in removing dyes from aqueous solutions. Many kinds of adsorbents for various applications have been developed and commercialized. In general, these adsorbents are highly porous particles having adequate surface area for adsorption. However, they are some limitations. In the case of anionic dyes as these biomaterials contain negatively charged cellulosic moieties, lower adsorption is resulted from coulombic repulsion. In addition, the existence of intraparticle diffusion may lead to a decrease in the adsorption rate and lowering macromolecules' availability capacity. Therefore, to develop an adsorbent with large surface area and small diffusion resistance has significant importance in practical use.

Various natural materials are attractive adsorbents, such as chitosan and montmorillonite. They have high adsorption capabilities for various kinds of dyes materials. Chitosan, a biopolymer of glucosamine, showed a higher colour adsorption capacity in comparison to activated carbon. Chitosan can also reduce dye concentration to ppb levels (Gurses et al, 2004). However, using pure chitosan as an adsorbent illustrates several disadvantages such as low surface area, low specific gravity, high cost, and weak chemical and mechanical properties (Chang, and Juang, 2004). Therefore, chitosan is chemically or physically modified to improve its practical applications.

Montmorillonites, natural clay minerals are low-cost materials due to their abundance in most continents of the world. They possess layered structures which act as host materials with high adsorption properties. Clays themselves possess the high adsorption capabilities, the modification of their structure can successfully improve their capabilities (Ozdemir et al, 2003). Adsorption of chitosan on montmorillonite, results in structures with good adsorption properties for anions because the  $-\text{NH}_3^+$  groups which are not directly involved in the interaction with the clay surfaces can act as anionic exchange sites (Darder et al. 2003). Accordingly, montmorillonite–chitosan bionanocomposites have recently been proposed for anion-adsorption related applications, such as in the development of potentiometric sensors for anions or for the removal of selenate and tannic acid from water (An. and. Dultz. 2007; Bleiman and Mishael, 2010; Darder, 2005)

Chitosan, a biopolymer of glucosamine, showed a higher capacity for adsorption of colorant than activated carbon (Oscan and Osacan, 2003). Pathavuth and Punnama (2009) demonstrated that chitosan montmorillonite exhibit superior adsorption capacity compared with chitosan  $\text{Na}^+$  montmorillonite. Aleksandra (2012) studied the sorption of Bezactiv Orange V-3R onto chitosan/montmorillonite membranes and reported the high potentials for dyes adsorption. Li and Ai qin et al (2007) studied chitosan/montmorillonite with the molar ratio of CTS to MMT of 5:1 showed good adsorption for Congo red. dye, and reported that the adsorption capacities of the Congo red chitosan/montmorillonite are higher than chitosan. Siriwan et al (2007) reported that three factors, (i) pH of dye solution in the range of 4–6, (ii) increasing the mMMT ratio and (iii) the amount of adsorbent to dye ratio, improved the adsorption efficiency.

In this work we attempt to utilize CMMt for adsorption Congo red in column systems. The effect of influent concentration, bed height and flow rate on column performance and the shape of the breakthrough curves were evaluated. Adams–Bohart, Thomas and Yoon and Nelson models were applied to the experimental data to evaluate the dynamic performance of the adsorption process and to assist in predicting the breakthrough curves. Regeneration of the chitosan bead was also conducted using  $0.1 \text{ molL}^{-1}$  HCl to assess whether the biomass was able to be efficiently regenerated and reused.

## EXPERIMENT

### Materials

The dye Congo red, CI acid red 87,  $\lambda_{\text{max}} = 517 \text{ nm}$ . Sodium tripolyphosphate, sodium hydroxide, was supplied by Sigma Co and used as received. Glacial acetic acid and hydrochloric acid were of analytical grade. Chitosan DD 90 was purchased from Material Science Research Centre, BATAN, Jakarta and montmorillonite from Laboratory Petrologi, Trisakti University of Jakarta.

### Preparation of Chitosan-Montmorillonite (Chi-MMT)

Chitosan solution was prepared by dissolving 4 g of chitosan in 196 mL of 2% v/v acetic acid. The pH of chitosan solution was adjusted to 4.9 with 1 M NaOH. The solution was left overnight before was slowly added into a suspension bath containing 100 ml montmorillonite 2.50% (w/v). The mixture was treated at  $60^\circ\text{C}$  for 24 h. The chitosan intercalated MMT (Chi-MMT) was washed with distilled water until the pH of the washed water became neutral. Chi-MMT was separated from water by centrifugation at 3500 rpm for 10 min and then dried at  $60^\circ\text{C}$  for 48 h.

### Characterization of the Chi-MMT

The prepared sorbents were characterized by Fourier Transform Infrared Spectroscopy (FTIR). FTIR spectra of the samples as solid by diluting in KBr pellets were recorded with JASCO-460 plus model. The results of FTIR spectroscopy was used to confirm the functional groups present, before and after Congo red sorption onto the sorbents

## Experimental Procedures

### Adsorption Experiments

Stock Congo red solution of 500ppm was prepared using Congo red with deionized water. For further experiments, solutions of 50 ml volume were prepared by dilution of this stock. Batch tests were conducted in 100 ml stoppered flasks in a water bath kept at 298K. Agitation rate was held constant at 120 rpm. The pH of the solutions was regulated by micro-additions of 0.1 M HCl and 0.1M NaOH. Isotherm data were obtained by placing 100 mg Chi-MMT in Congo red solutions of different initial concentration (200–1000mg l<sup>-1</sup>). Concentration was monitored with respect to time for kinetic analysis. The concentration of the samples was analyzed spectrophotometrically (Shimadzu UV 160) at 540 nm.

### Column Adsorption Model

Sorption in a continuous-flow system was done in a fixed bed column reactor (2.0cm i.d., 30 cm column length). Each bed of sorbent of desired height was underlain by 4 cm<sup>3</sup> of glass wool and 6 cm<sup>3</sup> of 3mm glass beads. The addition of glass wool and glass beads was made to improve the flow distribution. The schematic diagram of the reactor is shown in Figure 1. Congo red solution having an initial concentration of 400 mg l<sup>-1</sup> was adjusted to pH 5.5 was passed through a column at a fixed flow rate. Samples were collected from the exit of the column at different time intervals and analyzed for Congo red using spectrophotometer (Shimadzu 160A). Operation of the column was stopped when the effluent concentration of Congo red exceeded a value of 395 mg/l.



Figure 1: Small Column for Fixed Bed Studies

### Effect of Mass Sorbent

The effect of varying the mass sorbent (0.3 g and 0.5 g) on the column parameters were studied. The flow rate of 0.3 mL/min and initial influent concentration of 400 mg/L were kept constant.

### Effect of Flow Rate

Different flow rates of 0.2 mL/min, 0.4 mL/min, and 0.6 mL/min were used and the effect on the column performance was analyzed. The initial inlet concentration 400 mg/L and mass sorbent were maintained at 0.5 g, respectively. The flow rates were selected based on the typical range of groundwater velocity.

### Thomas' Model

Thomas model were used to fit the data obtained from the fixed-bed experiments. Thomas' model (Eq. 1) enables us to easily ascertain, in an adsorption bed, the operational parameters for maximum adsorption capacity  $q_0$  (mg/g), and the

velocity constant  $k_{Th}$  (mL/mg min). Where  $C_0$  is the feed concentration in mg/L,  $C_t$  is the exit concentration in effluent in mg/L,  $Q$  is the flow rate in mL/min,  $V_{eff}$  the volume treated in L, and  $W$  the adsorbent mass in g, Thomas' model has this form:

$$\ln\left(\frac{C_0}{C_t} - 1\right) = \frac{k_{Th} Q_0 W}{Q} - k_{Th} C_0 t \quad (1)$$

This model is one of the most general and widely used theoretical methods to describe column performance. The Thomas or reaction model, which assumes Langmuir kinetics of adsorption-desorption and no axial dispersion is derived with the assumption that the rate driving force obeys second-order reversible reaction kinetics. Thomas' solution also assumes a constant separation factor applicable to both favourable and unfavourable isotherms [14]. Adsorption is usually not limited by chemical reaction kinetics but it is often controlled by interphase mass transfer. This discrepancy can lead to some error when this method is used to model adsorption process (Aleksandra et al, 2012; Li and Ai Qin, 2007).

### Regeneration of the Column

The column bed was then rinsed by passing 100 ml deionised water in upward direction at the same speed as used for biosorption from the Congo red solution. Desorption was carried out by passing 0.01M NaOH through the column bed in upward direction at a flow rate of 10 ml min<sup>-1</sup>. The effluent metal solution was collected and was analyzed for ion Congo red content. On the completion of desorption cycle, the column was rinsed with deionised water in the same manner as for biosorption till the eluting deionised water attained pH 7.0. The desorbed and regenerated column bed was reused for next cycle.

## RESULTS AND DISCUSSIONS

### Characterization of MMT

#### XRD Analysis

Nanocomposites was analysed by XRD and the powder patterns are presented in Figure 2. A typical diffraction peak of MMT is 7.08°, responding to a basal spacing of 12.46 Å. After intercalation with chitosan, this peak disappears. The movement of the typical diffraction peak of MMT to lower angle (5.18°) responding to a basal spacing of 17.04 Å indicates the formation of the flocculated-intercalated nanostructure with the molar ratios chitosan to MMT of 1:5. It is reported that the formation of flocculated structure in Chi-MMT nanocomposites is due to the hydroxylated edge-edge interaction of the silicate layers (Li and Ai Qin, 2007).

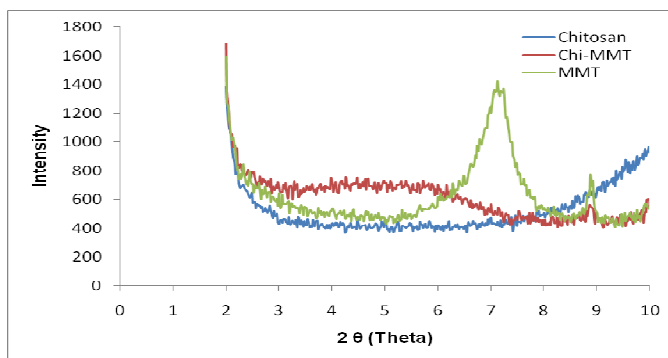


Figure 2: XRD Patterns of The Chitosan (a), Montmorillonite (b) and Chi-MMT(c)

#### FTIR Analysis

The FT-IR spectrum of MMT (Figure 3) shows the vibration bands at 3460-3640 cm<sup>-1</sup> for O-H stretching,

3442  $\text{cm}^{-1}$  due to interlayer and intralayer H-bonded O–H stretching, 1640  $\text{cm}^{-1}$  for H–O–H bending, 1113 and 1035  $\text{cm}^{-1}$  for Si–O stretching, 935 and 915  $\text{cm}^{-1}$  for Al–OH, and 797  $\text{cm}^{-1}$  due to (Mg–OH) vibration modes and 520 and 467  $\text{cm}^{-1}$  for Si–O binding.

While the spectrum of chitosan(Fig 3) showed peaks at 3000-3750  $\text{cm}^{-1}$  due to the overlapping of O–H and N–H stretching bands, 2920  $\text{cm}^{-1}$  for aliphatic C–H stretching, 1634 and 1594  $\text{cm}^{-1}$  for N–H bending, 1420 and 1382  $\text{cm}^{-1}$  for C=O bending, 1151 and 1079  $\text{cm}^{-1}$  for C–O stretching.

The spectrum of the Chi-MMT shows the combination of characteristic absorptions due to the chitosan and MMT groups. The peak at 1594  $\text{cm}^{-1}$  of the –NH<sub>2</sub> group in the starting chitosan was shifted to 1520  $\text{cm}^{-1}$  in the Chi-MMT spectrum, corresponding to the deformation vibration of the protonated amine group (–NH<sub>3</sub><sup>+</sup>) of chitosan. This –NH<sub>3</sub><sup>+</sup> group interacts with the negatively charged sites of MM

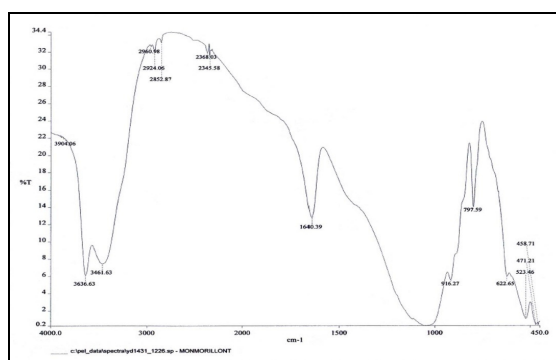


Figure 3: FTIR Spectrum MMT

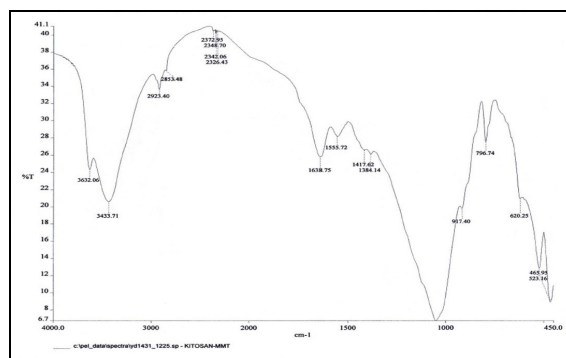


Figure 4: FTIR Spectrum Chitosan

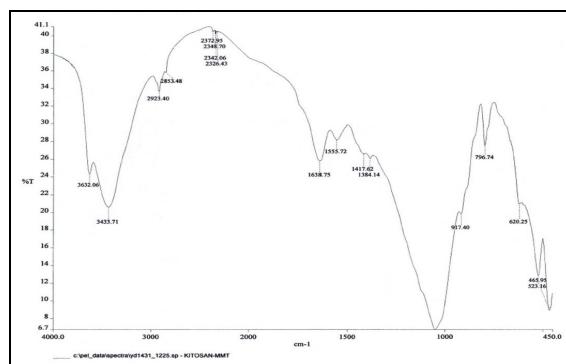
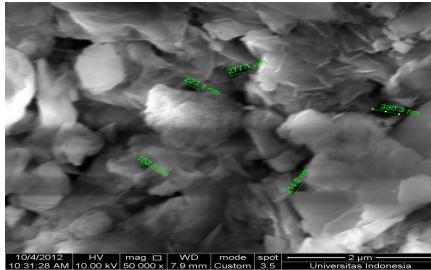


Figure 5: FTIR Spectrum Chi-MMT

The FESEM patterns of Chi-MMT are presented in Figure 6. It Shows Chi-MMT having a shape resembling a circle with different size and pore size range between 152.5 nm until 380.3 nm with existence of pore on Chi-MMT is expected to increase its ability in adsorbing Congo red.



**Figure 6: FESEM Pattern of Chi-MMT**

### Adsorption Isotherms

The relationship between adsorbed metal concentration and concentration of the solution at equilibrium is described by isotherm models, of which Langmuir and Freundlich are the most

widely referred equations. Langmuir isotherms is expressed as :

$$\frac{1}{q_e} = \frac{1}{q_m} + \frac{1}{bq_m C_e} \quad (2)$$

Here,  $q_e$  is the equilibrium adsorption capacity ( $\text{mg g}^{-1}$ ),  $C_e$  is the equilibrium concentration of solution ( $\text{mg l}^{-1}$ ),  $q_m$  is the Langmuir constant representing the maximum adsorption capacity ( $\text{mg g}^{-1}$ ) and  $b$  is the Langmuir constant related to the energy of adsorption ( $\text{l}^{-1} \text{mg}$ ). The values of Langmuir constants  $q_m$  and  $b$  were obtained from the intercept and slope of the plot between  $(1/q_e)$  vs.  $(1/C_e)$ . The linearization of the equations for Chi-MMT, are  $y = 0.01834x - 0.0843$ , and the values of  $R^2 = 0.999$ , respectively. The  $q_m$  values for the adsorption of Congo red by Chi-MMT were  $49.80 \text{ mg g}^{-1}$  respectively, which are sam as the experiment data  $46.70 \text{ mg g}^{-1}$

Contradictory to Langmuir, Freundlich Freundlich isotherm is expressed as

$$\text{Log } q_e = \text{log } K_F + (1/n) \text{ log } C_e \quad (3)$$

where  $K_F$  and  $n$  are constants for Freundlich isotherm that are indicative of the adsorption capacity ( $\text{mg g}^{-1}$ ) and intensity of the adsorbent, respectively. The values of  $K_F$  and  $n$  were calculated from the slope and intercept of the plot between  $\ln q_e$  and  $\ln C_e$ . The linearization of the equations for Chi-MMT, are  $y = 0.01834x - 1.0843$ , and the values of  $R^2 = 0.889$ , respectively. The  $K_F$  values for the adsorption of Congo red by Chi-MMT were  $4.30 \text{ mg g}^{-1}$  and  $n=1.26$  respectively

### Adsorption Kinetics

Two simplified kinetic models including pseudo-first-order and pseudo-second-order equations are analysed. A simple kinetic model that describes the process of adsorption is the pseudo-first-order equation. It was suggested by Lagergren (2000) for the adsorption of solid/liquid systems and its formula is given As

$$\log(q_e - q_t) = \log q_e - \frac{k_1 t}{2.303} \quad (4)$$

Pseudo-second-order model is based on adsorption equilibrium capacity can be expressed as :

$$\frac{t}{qt} = \frac{1}{k_2 q^2 e} + \frac{t}{qe} \tag{5}$$

where  $k_2$  ( $\text{g mg}^{-1} \text{min}^{-1}$ ) is the rate constant of the pseudosecond- order adsorption. The linear plots of  $\log(qe - qt)$  versus  $t$  and  $(t/qt)$  versus  $t$  drawn for the pseudo-first-order and the pseudo-second-order models, respectively. The rate constants  $k_1$  and  $k_2$  can be obtained from the plot of experimental data. The correlation coefficients ( $R$ ) of the pseudo-first-order model are 0.901, respectively. For the pseudo-second-order model, the correlation coefficients ( $R$ ) are 0.986, respectively. Therefore, the adsorption of congo red on Chi- MMT were better described by the pseudo second- order rather than by the pseudo-first-order. This result also indicates that the adsorption rate of dye depends on the concentration of dye at the absorbent surface and the absorbance of these absorbed at equilibrium [16].

**Breakthrough Profiles**

The sorption of Congo Red onto CMMt in fixed-bed systems was investigated as a function of flow rate and mass sorbent . The operating parameters given by the applied models, the adsorption characteristics of the column were reported in terms of the volume,  $V_b$ , and the column capacity,  $q_b$ , at the breakthrough point; the volume,  $V_e$ , and the column capacity at exhaustion point,  $q_e$ . The breakthrough point was defined as the point at which the effluent concentration was equal to 0.05 $C_0$ , while the exhaustion point was defined as the point at which the effluent concentration reached a value of 0.90  $C_0$ .

**Influence of Bed Height (Amount of Sorbent)**

An increase in mass of CMMt (the height of the bed ) increases the contact time between the dye and chitosan. It also increases the quantity of surface area of adsorbent, which provides more binding sites for adsorption. This was expected to affect breakthrough. However, by plotting the breakthrough curves as a function of the bed volumes, the influence of the geometry of the column was eliminated, enabling better comparison of the different curves. Figure 7 shows the experimental breakthrough curves for Congo red for two different CMMt masses. All three curves had a similar shape. However, after the breakthrough point they became slightly steeper as the mass of the CMMt increased. As indicated in Tables 1, the mass sorbent has a great effect on the column performance, as inferred from the variation in the values of the experimental and model parameters. This influence is expected in the case of low porous sorbents for which the intraparticle diffusion is the limiting step. The experimental parameters,  $V_{eff}$ ,  $q_b$  and  $q_e$ , increased when the mass sorbent increased.

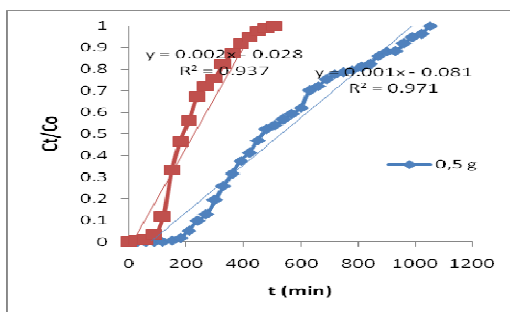


**Figure 7 : Effect of Mass Sorbent (G) on Breakthrough Curves for Removal Congo Red by Chi-MMT Initial Concentration of Congo Red = 400 mg/L and Flow Rate 0.2 mL/min**

**Table 1: Column Data and Parameters Obtained for Chi-MMT**

Flow Rate mL/min	V <sub>eff</sub> (mL)	ΔT (Menit)	q <sub>e</sub> (mg/g)	q <sub>b</sub> (mg/g)
0.2	210	1050	25.92	15.68
0.4	240	600	17.28	14.72
0.6	360	360	20.01	13.04
Mass Sorbent				
0.3	102	510	15.36	12.37
0.5	210	1050	25.92	15.68

### Effect of Flow Rate

In column studies, the contact time is the most significant variable and therefore mass adsorbent and solution superficial velocity are the main parameters. Consequently, the effect of superficial flow rate on Congo red sorption onto CMMt was examined by varying the superficial flow rate from 0.2 to 0.6 ml/min, while the CMMt mass and the initial concentration of Congo red were held constant at 0.5 g and 400 mg L<sup>-1</sup>, respectively. The breakthrough curves are illustrated in Figure 8. The curves show that the adsorption of Congo red onto CMMt depends on the superficial flow rate. The breakthrough curves became steeper and shifted to the origin with increasing superficial flow rate. At high flow velocities and short beds, the sorbent becomes less saturated due to a lower contact time. The influence of mass transfer limitations appears later, allowing a better modelling of the curves. For the lowest flow velocity studied, the uptake at exhaustion was equal to the maximum equilibrium capacity. However, the degree of sorbent usage was always lower than 50%, due to the spread shape of the curves.

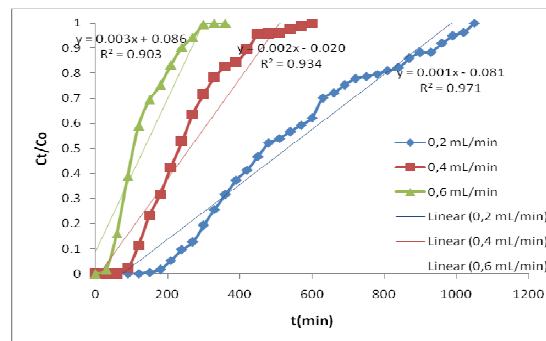


**Figure 8 : Effect of Flow Rate (ML/Min) on Breakthrough Curves for Removal Congo Red by Chi-MMT Initial Concentration of Congo Red = 400 mg/L and Mass Adsorbent 0.5 g**

### Breakthrough Curve Modelling

Several mathematical models have been developed for describing and analyzing lab-scale column studies for the purpose of industrial applications. In this study, the Adams–Bohart, Thomas and Yoon models were used to identify the best model for predicting the dynamic behaviour of the column. The Thomas model is one of the most widely used models to describe the performance theory of the sorption process in a fixed-bed column. This model assumes that Langmuir kinetics of adsorption–desorption and no axial dispersion are derived with the assumption that the rate driving force obeys second-order reversible reaction kinetics (Thomas, 1944).

To determine the maximum adsorption capacity ( $q_0$ ) at different mass sorbent and flow rate in column, the data were fitted to the Thomas equation model by using linear regression analysis. Table 2 illustrates the model constant ( $k_{th}$ ),

maximum adsorption capacity ( $q_0$ ) and correlation coefficient for CMMt. The  $k_T$  and  $q_0$  value were calculated by plotting  $\ln(C_t/C_0 - 1)$  against 't' using values from the column experiments. From Table 2, Figure 7 and Fig 8, that the model gave a good fit for the experimental data obtained for CMMt. It can be seen that as flow rate increased, the value of  $k_T$  increased whereas the value of  $q_0$  showed a reverse trend. With mass adsorbent increasing, the value of  $k_T$  decreased and the value of  $q_0$  increased.

**Table 2: Parameters Predicted from Thomas Model for Chi-MMT**

Flow Rate mL/min	$k_{TH}$ (L/Minit ·g)	$q_0$ (mg/g)	$R^2$
0.2	0,0000200	99,62	0.8532
0.4	0,0000425	90,73	0.8445
0.6	0,0000700	65,59	0.9313
Mass Sorbent			
0.3	0,0000475	65,3614	0.941
0.5	0,0000200	99,62	0.8532

From Table 2, the values of  $k_{Th}$  became bigger with the flow rate increasing while the values of  $q_0$  became bigger with initial dye concentration increasing. With the mass sorbent increasing, the values of  $k_{Th}$  became smaller while the value of  $q_0$  increased. Adsorption capacity depended mainly upon the amount of the adsorbent available for adsorption. The breakthrough time and exhaustion time increased with the increase in mass sorbent since more time was required to exhaust more adsorbent. But the slope of the breakthrough curve decreased as the bed height increased. This was due to an increase in the axial dispersion of the dye over the column with an increase in column height. This increase in bed height resulted in an increase in the volume of the dye solution treated and therefore a higher percentage of Congo red removal.

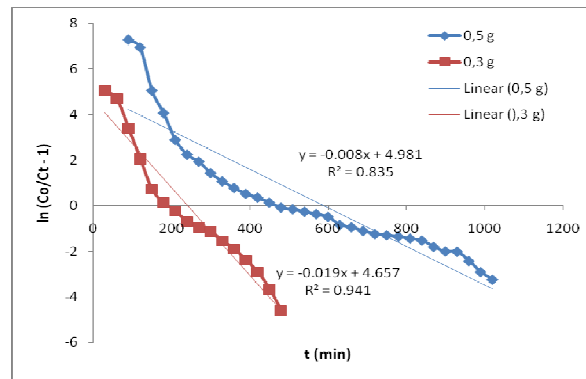


**Figure 9: Thomas Model Plot Chi-MMT for Mass Sorbent 0.3 g and 0.5 g at Flow Rate 0.6 mL/min**

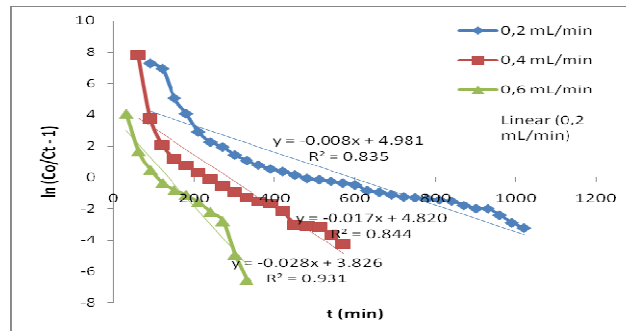


**Figure 10: Thomas Model Plot Chi-MMT for a Flowrate of 0.2, 0.4 and 0.6 mL/min and Mass Sorbent 0.3 g**

The Thomas equation coefficients for Congo red adsorption were  $KT = 0,0000700L/(min\ mg)$  and  $q_0 = 65,59\ mg/g$ . The value of  $q_0$  is a measure of the adsorption capacity at the Chi-MMT with mass sorbent 0.3 g and flow rate 0.6 mL/min. The theoretical predictions based on the model parameters are compared in Fig. 11 and Figure 12 with the observed data.

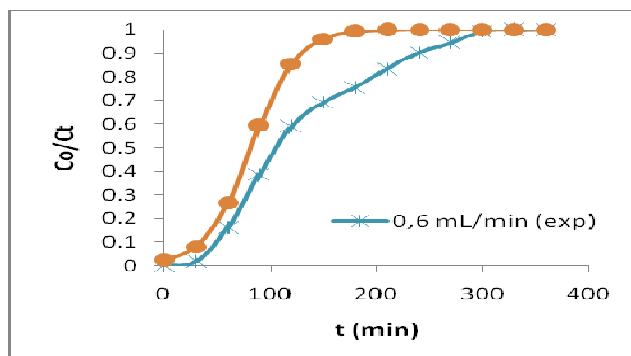


**Figure 11: Comparison of the Experimental and Predicted Breakthrough Curves According to Thomas Model (at 25 °C, pH 5 and C0 400 mg/L, Flow Rate 0.6 mL/min)**

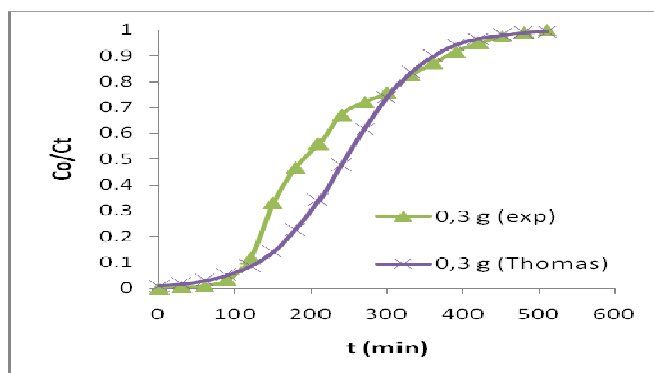


**Figure 12 : Comparison of The Experimental and Predicted Breakthrough Curves According to Thomas Model (at 25 °C, pH 5 and C0 400 mg/L, Mass Sorbent 0.3 g)**

### Column Regeneration

Reusability of the sorbent is of crucial importance in any industrial practice for dye removal from wastewater. This can be evaluated by comparing the sorption performance of regenerated biomass with the original biomass. In this study, Chi-MMT was reused for two sorption–desorption cycles at  $0.2\ mL\ min^{-1}$ . The column was packed with 0.5 g of Chi-MMt, an initial bed height of 1 cm and saturated with  $400\ mg\ L^{-1}$  initial Congo red concentration. Fig. 5 illustrates the desorption of eosin Y Chi-MMt at pH 12 with time. The desorption process is observed to be reasonably fast initially and then slowly to attain equilibrium after about 13 h. The Chi-MMt used in this study were reused for five cycles without any loss of their sorption

### CONCLUSIONS

A new and efficient Chi-MMt based bioadsorbent with increased thermal stability was synthesized and used for removal of Congo red from an aqueous solution in a fixed bed column. The results obtained showed that the sorption Congo red is dependent on mass sorbent, flow rate, and influent concentration. Longer breakthrough and exhaustion time occurred at a mass sorbent correlate to a lower flow rate and lower influent concentration. The Thomas model was

successfully applied to the experimental data obtained from dynamic studies performed on a fixed column. The model is able to predict the breakthrough curves and to determine the column kinetic parameters.

## ACKNOWLEDGEMENTS

Authors are grateful to State University of Jakarta for providing financial assistance to carry out this research work. This study was financially supported by Research Fund (No. 200 /VI/SPK/Lemlit/2010).

## REFERENCES

1. An.J.H., S. Dultz.S.2007. Adsorption of tannic acid on chitosan–montmorillonite as a function of pH and surface charge properties, *Appl. Clay Sci.* 36 : 256–264
2. Aleksandra R. Nesica, Sava J. Velickovic, Dusan G.2012. Antonovic. Characterization of chitosan/montmorillonite membranes as adsorbents for Bezactiv Orange V-3R dye. *Journal of Hazardous Materials.* 209 : 256– 263
3. Bleiman.N., and Y.G. Mishael.Y.G. 2010.Selenium removal from drinking water by adsorption to chitosan–clay composites and oxides: batch and column tests, *J. Hazard.Mater.* 183 : 590–595
4. Chang, M.Y., and Juang, R.S.2004. Adsorption of tannic acid, humic acid, and dyes from water using the composite of chitosan and activated clay. *Journal of Colloid and Interface Science.* 278: 18-25
5. Crini.N .2006. Non conventional low cost adsorbent for dye removal; a review.*Bioresour.Technol.* 97: 1061-1085
6. Darder.M., Colilla.M., Ruiz-Hitzky.E.2003. Biopolymer–clay nanocomposites based on chitosan intercalated in montmorillonite, *Chem. Mater.* 15: 3774–3780
7. Darder.M., M. Colilla.M., E. Ruiz-Hitzky.E..2005. Chitosan–clay nanocomposites: application as electrochemical sensors, *Appl. Clay Sci.* 28 : 199–208
8. Gurses, A., Karaca, S., Dogar, C., Bayrak, R., Acikyildiz, M., Yalcin, M.. 2004.Determination of adsorptive properties of clay/water system: methylene blue sorption. *J. Colloid Interface Sci.*269: 310–314
9. Li Wang and Aiqin Wang.2007. Adsorption characteristics of Congo Red onto thechitosan/montmorillonite nanocomposite. *Journal of Hazardous Materials.* 147 : 979–985
10. Lourenco.N.D.,Novais.J.M.,Pinheiro.H.M..2003. Reactive textile dye colour removal in a sequencing batch reactor.. *Water Science and Technology.* 42: 321-328
11. Oscan.A.S., and .Oscan.A.2004. Adsorption of acid dyes from aqueous solution onto acid activated bentonite. *J.Coll.interface Sci.* 276 : 39-44
12. Ozdemir, O., Armagan, B., Turan, M., Celik, M.S.2003. Comparison of the adsorption characteristics of azo-reactive dyes on mesoporous minerals. *Dyes Pigm.* 2004, 62: 49–60
13. Pathavuth Monvisade, Punnama Siriphannon.2009. Chitosan intercalated montmorillonite: Preparation, characterization and cationic dye adsorption.*Applied Clay Science.* 42: 427-431
14. Pearce, C.I., Lloyd, J.R., Guthrie, J.T.2003. The removal of colour from textile wastewater using whole bacterial cells: a review. *Dyes Pigm.* 58:179–196
15. Siriwan Kittinaovarat, Panida Kansomwan, Nantana Jiratumnukul. 2010. Chitosan/modified montmorillonite beads and adsorption Reactive Red 120. *Applied Clay Science.* 48: 87–91
16. Sun.S.L., and Wang.A.Q.2006. Adsorption kinetics of Cu(II) ions using *N,O*-carboxymethyl-chitosan, *J. H.S.Lazard. Mater.*2006, 131: 103–111
17. Thomas.H.C.1944. Heterogeneous ion exchange in a flowing system, *J. Am. Chem. Soc.* 19 66 : 1664–1666

